Pb–Pb age of limestones of the Middle Riphean Malgina Formation, the Uchur–Maya Region of East Siberia

Article *in* Stratigraphy and Geological Correlation · November 2001

CITATIONS
39

READS
89

7 authors, including:

Igor Gorokhov
Russian Academy of Sciences
122 PUBLICATIONS **2,263** CITATIONS
SEE PROFILE

O. K. Kaurova
12 PUBLICATIONS **252** CITATIONS
SEE PROFILE

V. N. Podkovyrov
Russian Academy of Sciences
113 PUBLICATIONS **1,885** CITATIONS
SEE PROFILE

Stratigraphy and Geological Correlation, Vol. 9, No. 6, 2001, pp. 527–539. Translated from Stratigrafiya. Geologicheskaya Korrelyatsiya, Vol. 9, No. 6, 2001, pp. 3–16.

Pb–Pb Age of Limestones of the Middle Riphean Malgina Formation, the Uchur–Maya Region of East Siberia

G. V. Ovchinnikova*, M. A. Semikhatov, I. M. Vasil'eva*, I. M. Gorokhov*, O. K. Kaurova*, V. N. Podkovyrov*, and B. M. Gorokhovskii***

**Institute of Precambrian Geology and Geochronology, Russian Academy of Sciences, nab. Makarova 2, St. Petersburg, 199034 Russia*

***Geological Institute, Russian Academy of Sciences, Pyzhevskii per. 7, Moscow, 109017 Russia*

Received December 25, 2000

Abstract—The carbonate Malgina Formation, a constituent of the Riphean hypostratotype in Siberia, corresponds, according to paleontological evidence, to the terminal Middle Riphean horizons, and present-day geochronological data indicate that it is younger than 1300 ± 5 Ma and older than 1025 ± 40 Ma. Eight limestone samples (Mg/Ca < 0.066) selected for the Pb–Pb age determination contain less than 5.8% of silicate components and are insignificantly altered, as it is evident from geochemical criteria (Mn/Sr ≤ 0.2, Fe/Sr ≤ 5, Rb/Sr ≤ 0.001) and minimum difference between $^{87}Sr/^{86}Sr$ ratios (≤0.0007) measured in the primary and secondary carbonate phases. Secondary carbonates were removed using the step leaching of samples in HBr of variable concentration. The Pb–Pb age of 1043 ± 14 Ma (MSWD = 7.8) that is calculated for 18 data points characterizing various carbonate phases appears to be best approximating the time of early diagenesis in the Malgina limestones. With due account for stratigraphic position of studied samples, this and other Pb–Pb dates obtained for the Middle–Upper Riphean carbonate formations of the Urals and Siberia are concordant with ages measured by other methods and form altogether a regular series of five successive values. The Pb–Pb isochron dates of stratigraphic significance can be obtained only after a strict procedure of sample selection followed by the removal of secondary carbonate phases with the help of step-leaching method.

Key words: U–Pb systematics, carbonate rocks, epigenesis, Middle Riphean, Upper Riphean, Siberia, Urals.

Until the recent time, geochronological characterization of the Riphean hypostratotype in the Uchur–Maya region of East Siberia was limited by K–Ar dates obtained more than 30 years ago for mineralogically unstudied glauconite (*Geochronologiya dokembriya...*, 1968; Semikhatov and Serebryakov, 1983; and references therein). Dates obtained by modern methods have been published recently only for the upper Ui and Lakhanda groups of the Uchur–Maya section (Rainbird *et al.*, 1998; Semikhatov *et al.*, 2000). These results considerably changed the traditional view of isotopic ages characterizing not only the upper horizons of the section, but also the boundary between the Middle and Upper Riphean. Reliable dates obtained recently for older horizons of the section define the maximum age limit of the Kerpyl Group (Khudoley *et al.*, 1999, 2001) that predates the Lakhanda Group unconformably overlying it.

In this study, we had two objects in view. First, it was purposeful to determine the precision Pb–Pb dates for limestones of the Malgina Formation of the Kerpyl Group in order to broaden geochronological characteristics of the Riphean hypostratotype in the Uchur–Maya region. Second, the comparison between these and other Pb–Pb dates known for other Riphean formations of the Urals and Siberia (Ovchinnikova *et al.*, 1995, 1998, 2000; Semikhatov *et al.*, 2000) offers a possibility to evaluate the resolution ability of the Pb–Pb method and stratigraphic potential of corresponding age determinations for the Upper Precambrian carbonate rocks.

GEOLOGICAL POSITION AND AGE OF STUDIED SAMPLES

There are two different Riphean structures in the Uchur–Maya region (Fig. 1): the stable Uchur–Maya plate in the west and the Yudoma–Maya trough in the east that actively developed (Nuzhnov, 1967; Semikhatov and Serebryakov, 1983; Shenfil', 1991). These paleostructures with contrastingly dislocated Upper Precambrian and Cambrian beds (subhorizontal in the plate and deformed into large open folds in the trough, where they are complicated by faults and thrusts) also differ in thickness, accumulation environments, and, to a certain extent, in composition of coeval formations. The regional succession of Riphean deposits includes five groups separated by unconformities of variable significance (Semikhatov and Serebryakov, 1983; Shenfil', 1991). The basal Uchur Group spans the Lower Riphean interval. The overlying Aimchan and Kerpyl

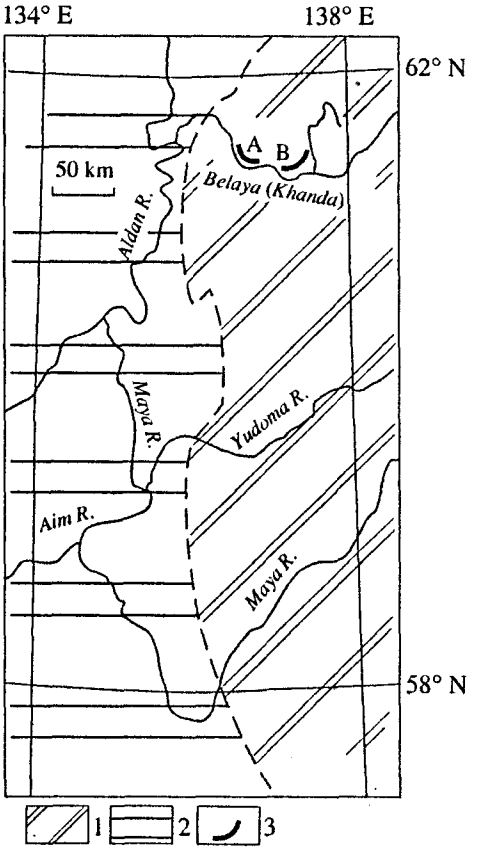

Fig. 1. Structural scheme of the Uchur–Maya region and localities of studied sections of the Malgina Formation: (1) Yudoma–Maya trough; (2) Uchur–Maya plate; (3) localities studied near the mouth of the Kurun-Mastakh Creek (A) and upstream off the Svetlyi Creek mouth (B), the right side of the Belaya River.

groups belong to the Middle Riphean, and the Lakhanda and Ui groups, which are terminal in the succession, correspond to the lower Upper Riphean.

The Kerpyl group that discordantly overlies either the older Riphean deposits, or the pre-Riphean crystalline basement, includes conformable beds of three subdivisions: the Totta Formation of siliciclastic sediments (450–1100 m thick), Malgina Formation of limestones (60–420 m thick), and Tsipanda Formation of dolomites (190–450 m thick). Samples studied in this work have been collected from two sections of the Malgina Formation, which are situated at the eastern and western limbs of the Gornostakhskii anticline in the northeast of the Yudoma–Maya trough and have been examined in coastal outcrops of the Belaya River (Fig. 2). The detailed description of both sections has been published earlier (Semikhatov and Serebryakov, 1983), and we present here only their general characteristics.

At the western anticline limb, we examined the Malgina deposits near the mouth of the Kurun-Mastakh Creek at the right side of the Belaya River. An upper part of the formation that is exposed here is about 70 m thick. It is composed of dark gray to gray fine-grained limestones displaying the microbial or fine horizontal lamination. The rocks have an insignificant amount of insoluble residue (0.5–4.5%). Along the contact with the overlying Tsipanda Formation, they are irregularly dolomitized at the epigenetic stage down to the depth of 50–55 m. Below this zone, limestones retain their original sedimentary textures and structures, being nonuniformly recrystallized into microsparite within small areas, which exhibit rare and diffuse patches of sparite and veinlets of secondary calcite. The underlying part of the formation (300–330 m thick) that is exposed upstream of the indicated site is predominantly composed of micrites intercalated with variably abundant interlayers of microbialites, calcisiltite, and rarer flakestone. Near the base, there are interlayers of clayey limestone and laminae of shale. Coloration of this rock succession gradually changes from dark gray in the upper part to pale-yellow and greenish gray in the middle one, and then to pinkish gray and cherry-red near the base. All the listed rocks are slightly recrystallized (small dispersed patches of microsparite and widely spaced calcite veinlets).

At the eastern limb of the Gornostakhskii anticline (Belaya River banks upstream off the Svetlyi Creek mouth), the Malgina Formation is up to 420 m thick. Its basal member (40–42 m thick) is composed of greenish gray, pinkish, and pale-yellow flaggy limestones having fine microbial lamination and intercalated with fine laminae (1–3 mm) of greenish gray shale. Near its base, there are, in addition, interlayers of clayey limestone and marl. The content of siliciclastic fraction varies in these rocks from 7.3 to 13%. Greenish to pale-yellow beds of micro-grained limestones above this member are 140–160 m thick in total. They enclose laminae of pale-yellow microbial limestones. The formation section is crowned with the 220-m-thick succession of dark gray bituminous micrites, which contain an insignificant siliciclastic admixture (0.6–2.2%) and locally enclose thin lentils of black cherts. Outside the zone of secondary dolomitization, all rocks of the Malgina Formation show micritic and subordinate microsparitic textures. Patches and veinlets of secondary recrystallization are scarce. Micritic limestones do not exhibit cathodoluminescence. Microsparites show a weak nidal luminescence within carbonate veinlets.

In the Yudoma–Maya trough, the Malgina sediments accumulated in the comparatively deep settings (below and above the storm wave base) of the distal shelf under condition of the quick rise and subsequent slow drop of sea level. Compositional changes in sediments suggest that the noticeable inflow of clayey material from the west into the basin took place at the very beginning of the Malgina time. By the end of this time, there were local anoxic environments in the basin, as it is evident from presence of rather thick (up to 5–10 m) packets of black limestones and clayey–calcareous shales enriched in organic matter, which appear near the for-

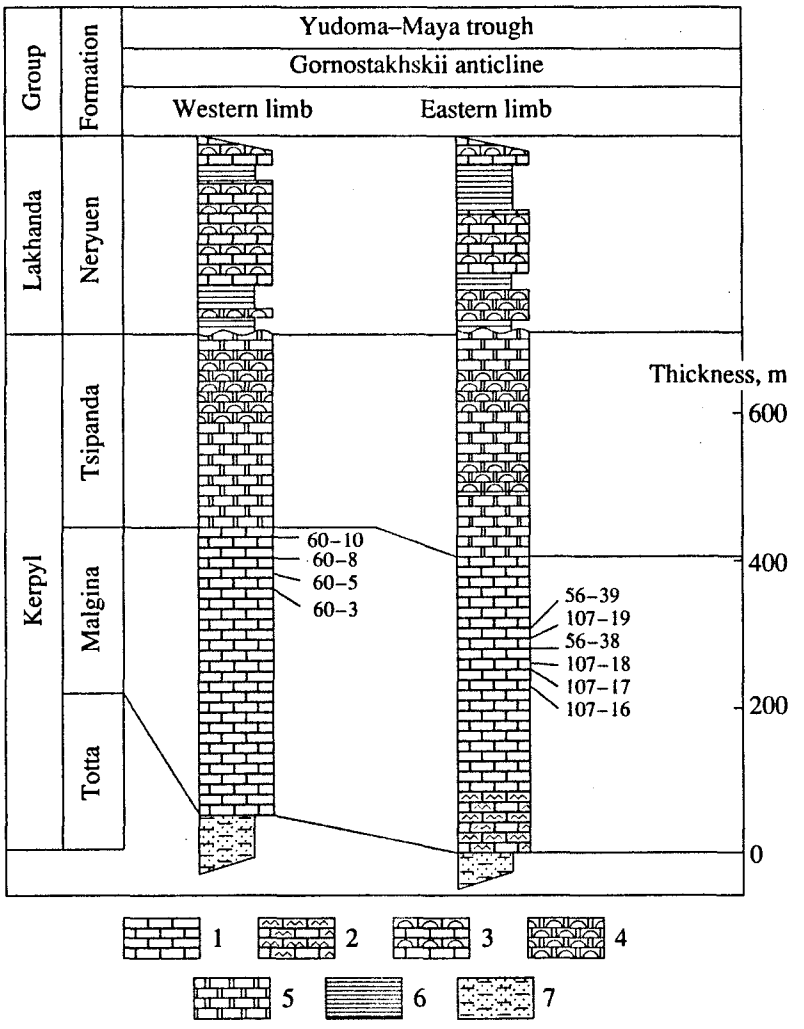

Fig. 2. Studied sections of the Malgina Formation with indicated sampling levels: (1) limestone; (2) microbial limestone; (3) stromatolitic limestone; (4) stromatolitic dolomite; (5) dolomite; (6) shale; and (7) siliciclastic rocks.

mation top in some sections of the Uchur–Maya plate and Yudoma–Maya trough (Semikhatov and Serebryakov, 1983). The maximum C_{org} content in such rocks (20.7–26.0%) is recorded in the Maya River middle courses (*Litologiya...*, 1980).

Age limits of the Kerpyl Group are established on the basis of paleontological, geochronological, and chemostratigraphic studies that yielded agreeable results.

Paleontological data point to an important compositional renewal of stromatolites and organic-walled microfossils across the Kerpyl–Lakhanda boundary. In addition to endemics, the Kerpyl Group encloses some transit Middle–Upper Riphean forms and rare taxa of stromatolites (*Omachtenia omachtensis* Nuzhn.) characteristic of the Lower Riphean Uchur Group. In addition, *Minjaria sakharica* Kom. et Semikh. and *Telemsina* sp. from the Kerpyl deposits are local representatives of form genera characteristic of the Upper Riphean in the Urals and North Africa. At the base of the Lakhanda Group, transit stromatolite taxa become much more diverse and associate with newcomers *Inzeria tjomusi* Kryl., *Jurusania cylindrica* Kryl., and *Baicalia lacera* Semikh., which are typical of the lower Upper Riphean horizons in several regions (Krylov, 1975; Semikhatov and Serebryakov, 1983; Semikhatov, 1995). Most remarkable among these taxa is *B. lacera* whose microstructure is also known as characterizing representatives of other morphotypes, which are widespread in the lower horizons of the Upper Riphean in many regions and mark the particular stage in evolution of cyanobacterial ecosystems and global environments of carbonate accumulation (Knoll and Semikhatov, 1998).

Much more impressive are compositional renewals in assemblages of organic-walled microfossils from the base of the Lakhanda group. Characteristic Upper Riphean forms appearing at this level are morphologi-

cally diverse acanthomorphic acritarchs *Trachyhystrichosphaera aimica* Herm., *T. stricta* Herm., and *Prolatoforma*; spiral-cylindrical *Obruchevella*; wide ribbons of *Plicatidium*; beaded *Arctacellularia*; fusiform *Pellicularia*; giant *Lakhandinia, Segmentothallus*, and *Eosolena*; remains of xanthophyte algae *Paleovaucheria*; thalluses of multicellular algae *Archaeoclada* and *Varioclada*; differentiated remains of lower fungi and their reproductive structures *Eosacchoromyces, Mucorites*, and others (Timofeev *et al.*, 1976; Yankauskas *et al.*, 1989; German, 1990; Veis *et al.*, 1998). These forms associate with abundant transit taxa inherited from the Totta Formation of the Kerpyl Group and deeper horizons of the section (Veis and Vorob'eva, 1992, 1993). Leaving aside simple representatives of these taxa, which are of negligible stratigraphic significance, we should mention others inherited from the Totta Formation, such as giant acritarchs *Chuaria*, tubercular *Pulvinosphaeridium*, elongated thalluses *Ostiana*, catenulate *Sphaerocongregus*, filamentous *Asperatofilum* and *Taenitrichoides*, multiserial sheaths *Polytrichoides* and *Eomicrocoleus*, branching thalluses *Ulophyton* and *Majaphyton*, and other complex and large morphotypes. Adverting to their morphology and size, some researches consider these forms as characteristic of the Upper Riphean (Veis *et al.*, 1998, 2000; and references therein). This viewpoint is however misleading, because all the organic-walled microfossils characterizing the Totta formation, have been found below the Upper Riphean deposits in the southern Urals and Cis-Uralian region (Veis *et al.*, 2000; *Stratigraphicheskaya skhema...*, 2000) and also in those deposits of the Anabar massif (Veis and Vorob'eva, 1993), which are of the Early Riphean age according to stromatolites and geochronological dates (Komar, 1966; Semikhatov and Serebryakov, 1983; Gorokhov *et al.*, 1991; 1997, 2001).

Available U–Pb dates of high precision define the age limits of the Riphean Kerpyl and Lakhanda groups of the Uchur–Maya region in a wide diapason only: the youngest population of clastic zircons separated from the Totta Formation is 1300 ± 5 Ma old (Khudoley *et al.*, 1999, 2001), whereas baddeleyite from diabase and gabbro-diabase sills in boundary horizons between the Lakhanda and Ui groups yielded the discordant age values of 1005 ± 4 and 974 ± 7 Ma (Rainbird *et al.*, 1998). Khudoley and his colleagues (2001) who analyzed the occurrence mode of these magmatic rocks concluded that they are localized in the lower part of the Ui Group and characterize the synsedimentary type of magmatism. Consequently, the aforementioned isotopic dates (1000–975 Ma) are likely to define the accumulation time of the lower Ui deposits. This conclusion is agreeable with the Pb–Pb date of 1057 Ma obtained for the youngest clastic zircon generation from these deposits (Rainbird *et al.*, 1998). The upper part of the Ui Group containing diabase fragments and discordantly overlain by Vendian strata is lacking reliable isotopic dates. At the same time, the Pb–Pb age of 1025 ± 40 Ma defines the time of early diagenesis for limestones from the lower part of the Lakhanda group (Semikhatov *et al.*, 2000). Accordingly, the Kerpyl group that is separated by the unconformable boundary from the Lakhanda group must be older than the latter age value.

Mineralogically unstudied glauconites from the Totta Formation that accumulated on the eastern, stably subsiding margin of the Uchur–Maya plate yielded the ordered series of K–Ar age values decreasing from 1170–1070 Ma in the lower formation part to 1070–1000 Ma in its middle interval, and then to 1020–970 Ma in the upper interval (*Geokhronologiya dokembriya...*, 1968; Semikhatov and Serebryakov, 1983). These dates have been traditionally regarded as indicating the accumulation (early diagenesis) time of the Totta sediments, but such an interpretation was doubted, when the U–Pb dates obtained for baddeleyite showed that the K–Ar dates for glauconites from the Lakhanda and Ui groups (960–870 and 760–700 Ma, respectively), which continued the aforementioned series of age values, are "rejuvenated." The considerable dispersion of age value characterizing the Totta glauconites suggests that K–Ar systems in some of these minerals were disturbed in the course of epigenesis. It should be added as well that Al-glauconites from lower and middle horizons of the Totta Formation sections in the Onmya Uplift located in the central part of the Uchur–Maya plate have experienced, according to their Mössbauer characteristics, the epigenetic structural transformations and yield the Rb–Sr isochron age of 864 ± 4 Ma that is distinctly "rejuvenated" (Semikhatov *et al.*, 1989). It is likely that the considerable age difference between glauconites collected from the Totta Formation in different areas of the Uchur–Maya plate is interrelated with variable geological history of individual areas. In any case, it is clear that the time range of the Kerpyl group is between 1300 ± 5 and 1025 ± 40 (1005 ± 4) Ma. At the same time, C-isotope chemostratigraphic data suggest that the Malgina Formation is younger than 1250 Ma, because important changes in the global biogeochemical cycle of carbon took place close to this date (Kah *et al.*, 1999; Bartley *et al.*, 2001): stasis of the global system that began 2060 Ma ago (Brasier and Lindsay, 1998) and was characterized by almost invariant $\delta^{13}C_{carb}$ values close to zero (0 ± 1.0 ‰ PDB) gave place to a period of their moderate variations from –2.0 to +3.0 ‰. In the Uchur–Maya region, this transition separates the Aimchan and Kerpyl groups. In the Aimchan carbonates, $\delta^{13}C$ values are close to 0.5 ± 0.6 ‰ and range in the Malgina limestones and their analogues of the Turukhansk area from –2.0 to +1.9 ‰ (Knoll *et al.*, 1995; Vinogradov *et al.*, 1998; Bartley *et al.*, 2001).

Thus, paleontological data suggest that the Kerpyl Group is terminal one in the Middle Riphean of the Uchur–Maya region. In addition, geochronological dates show that the basal Totta Formation of the group is younger than 1300 ± 5 Ma (U–Pb date for clastic zir-

cons). This formation presumably accumulated about 1170–1100 Ma ago (maximum K–Ar age of authigenic glauconite), whereas the overlying Malgina Formation is younger than 1250 Ma (C-isotope characteristics) and older than 1025 ± 40 Ma (Pb–Pb date for the lower Lakhanda limestones).

PROBLEMS OF U–PB AND Pb–Pb DATING OF SEDIMENTARY CARBONATE ROCKS

First attempts to determine the U–Pb and/or Pb–Pb age of carbonate rocks have been undertaken long ago (e.g., by Gerling and Iskanderova, 1976, for the Riphean carbonates of the Uchur–Maya region), but now they are of historical interest only because of a very low analytical level. The direct dating of marine carbonate deposits by U–Pb and Pb–Pb methods became possible much later, when the precision of mass-spectrometric measurements grew greatly and the level of laboratory contaminations was decreased down to the lowest notch (Moorbath *et al.*, 1987; Jahn and Cuvellier, 1994; Ovchinnikova *et al.*, 1995; and references therein). In the last decade, a considerable amount of Precambrian carbonate rocks was dated using these methods (Jahn *et al.*, 1990; Jahn and Cuvellier, 1994; Jahn and Simonson, 1995; Ovchinnikova *et al.*, 1995, 1998, 2000; Winter and Johnson, 1995; Russel *et al.*, 1996; Whitehouse and Russel, 1997; Toulkeridis *et al.*, 1998; Zachariah *et al.*, 1999). Nevertheless, some problems concerning the geochemical behavior of U and Pb in unmetamorphosed carbonate sediments restrict considerably their stratigraphic application.

The precision of U–Pb and Pb–Pb age determinations for dolomites and limestones directly depends on the variation diapason of initial U/Pb ratios in carbonate phases of these rocks. Magnitudes of these ratios are controlled by concentrations of both elements in sedimentation medium (seawater) and by distribution coefficients of U and Pb between carbonate minerals and seawater. The early diagenesis (the early dolomite formation after the high-Mg calcite included) results in redistribution of U and Pb between carbonate minerals and pore water: it usually decreases the content of U and increases concentration of Pb in carbonate sediments (Gobeil and Silverberg, 1989; Johnes *et al.*, 1992; Jahn and Cuvellier, 1994). As a result, the early diagenetic carbonates show much lower U/Pb ratios varying within a narrower range than in original carbonate sediments. Accordingly, the Pb–Pb ages of unmetamorphosed sedimentary carbonates mostly correspond to the resetting time of their U–Pb systems in the course of early diagenesis (Jahn and Cuvellier, 1994). At the same time, there are convincing sedimentological data (even for direct facies analogues of the Malgina carbonate rocks), which imply that the early diagenesis of Riphean carbonates was separated from their accumulation time by the geologically insignificant period (Maliva *et al.*, 1989; Petrov, 2000). Taking into consideration the analytical uncertainty, we may assume therefore that Pb–Pb ages obtained for Proterozoic limestones and early diagenetic dolomites are pretty close to the time of sedimentation.

The possibility of obtaining the stratigraphically significant U–Pb and Pb–Pb dates for Precambrian carbonate rocks is constrained by the following natural peculiarities of their U–Pb systems:

(1) Owing to the short residence time of Pb in seawater (Jahn and Cuvellier, 1994), the Pb isotope composition in the global ocean varies in space and with time depending on compositional changes in provenances.

(2) The irregular recrystallization of carbonate rocks at the early diagenetic stage may result in heterogeneity of Pb isotope composition in limestones and dolomites that could be perceptible on a scale of geological sampling.

(3) During the lithogenesis, carbonate minerals of sediments can be contaminated with U and/or Pb, which can be extracted from the associated silicate and sulfide admixtures, or mobilized by low-temperature fluids and meteoric waters from siliciclastic deposits present in the succession. Such a case is well exemplified by clayey limestones of the Upper Riphean Katav Formation of the Urals, which overlie the thick siliciclastic Zil'merdak Formation (Ovchinnikova *et al.*, 1998).

(4) As a rule, unmetamorphosed carbonate rocks of the Precambrian are to some extent inhomogeneous with respect to Pb isotope composition. The cause is that they all contain several carbonate phases, only one of which is early diagenetic, whereas others originated during the later stage (catagenetic in Russian and late diagenetic in English terminology) by interaction with media that had different Rb–Sr (Gorokhov *et al.*, 1995) and U–Pb systematics, i.e., different U and Pb concentrations and dissimilar Pb isotope compositions (Ovchinnikova *et al.*, 1995, 1998, 2000). One of the important factors of secondary alterations in carbonate rocks is their interaction with meteoric waters (Brand and Veizer, 1981; Banner and Hanson, 1990; Derry *et al.*, 1992; Gorokhov, 1996; Kuznetsov *et al.*, 1997; and references therein) that frequently leads to the U loss by carbonates, which become inappropriate for the U–Pb age determination (Asmerom and Jacobsen, 1993; Jahn and Cuvellier, 1994; Hoff *et al.*, 1995; Ovchinnikova *et al.*, 1995). At the same time, the resent Pb loss and the gain or loss of U do not change the Pb–Pb age of carbonates, and the last dating method has an advantage over the U–Pb method.

All the aforesaid implies that we should use first a complex of criteria to select the least altered samples of carbonate rocks potentially appropriate for the U–Pb and/or Pb–Pb dating. Afterward, we should extract the primary carbonate phases from those samples, which fit the selection criteria. Working with samples from the Malgina Formation, we used the published procedure of selecting the "best" samples (Ovchinnikova *et al.*,

1995, 1998, 2000; Vasil'eva *et al.*, 1998, 2000) on the basis of petrographic, geochemical, and isotopic criteria. Some deviations from this procedure are caused by specifics of the analyzed material (in particular, by absence of sulfide inclusions).

ANALYTICAL PROCEDURE

For the beginning, we sawed the macroscopically homogeneous limestone samples in two parts, one of which was used for chemical and isotopic analyses, and the other was examined by petrographic and cathodoluminescence methods. Petrography of the rocks was studied in thin sections. The cathodoluminescence characteristics are obtained using the "Camebax" microprobe at the Laboratory of Electronic Microscopy and Microanalysis of the "MEKHANOBR-ANALIT" Center, St. Petersburg. Chemical composition of rocks was analyzed at the Analytical Laboratory of the Geological Institute, Russian Academy of Sciences, using the atomic absorption spectroscopy for determination of Mn and Fe concentrations and wet chemical method for analysis of other components. In both cases, samples were dissolved in 1N HCl under the room temperature in order to leave intact the siliciclastic fraction of rocks.

According to results of chemical analysis, we selected 40 limestone samples among all others collected from the Malgina Formation, which had low content of silicate residue (≤13%) and Mg/Ca ratios ≤ 0.066. Petrographic and cathodoluminescent examination of these samples showed that they are lacking signs of significant epigenetic recrystallization and retain their primary textural and structural features. Only few samples from the western limb of the Gornostakhskii anticline, which exemplify upper horizons of the formation, turned out to be with microsparite patches visible against the general micritic background. Using then the strict geochemical criteria (Mn/Sr ≤ 0.2; Fe/Sr ≤ 5; Rb/Sr ≤ 0.001; Kuznetsov *et al.*, 1997), we selected 9 of these 40 samples, which appeared to be the least altered. The low alteration degree of finally selected rocks is also evident from data on their Rb–Sr systematics: the difference between the $^{87}Sr/^{86}Sr$ ratios, which were measured in leachates obtained after treatment of powdered samples in 1N ammonium acetate and in residues after leaching, turned out to be not greater than 0.0007. The only exception was Sample 60/8, for which this difference was 0.0011. In the selected samples, the content of insoluble residue usually ranged between 0.6 and 3.4% and never was greater than 5.8%, The residual fractions predominantly consisted of quartz and subordinate mica.

The non-cogenetic carbonate phases of different U–Pb systematics were separated using the three-step leaching procedure in HBr solution of various concentration under the room temperature. At the first stage, we treated the sample weighing during 30 minutes in 0.1N HBr, and 5 to 6% of the weighing entered the solution after this step. The carbonate phase that was leached at this stage is further designated as L-1. At the second stage, the first insoluble residue was treated again during 30 minutes in 0.25N HBr, and as a result, about 12% of its carbonate material entered the solution (phase L-2). The rest of carbonate material was finally dissolved during 24 h in 0.5N HBr (phase L-3). In the case of particular samples, we missed these treatment stages dissolving the bulk carbonate material in 1 N HCl to get the phase indicated as PCC-2. The silicate residue insoluble in HBr and HCl is indicated as the ISR phase. When it was necessary, we dissolved this residue in the mixture of concentrated HF and HNO_3.

Concentrations of U and Pb were analyzed using the isotope dilution technique and mixed $^{235}U + ^{208}Pb$ tracer. The Pb isotope composition was measured in aliquots without adding the tracer. U and Pb were separated from solutions using the ion-exchange technique with Bio-Rad 1 × 8 as described by Manhes *et al.* (1978). U and Pb isotope compositions were analyzed on Finnigan MAT-261 multicollector mass spectrometer using a regime of simultaneous measurement of all isotope ion currents. The measured Pb isotope ratios were corrected for the fractionation factor of 0.13% per atomic mass unit that was calculated from successive determinations of Pb isotope composition in NBS SRM-982 standard. The procedure blank during the period of our investigation was 0.05 ng for U and 0.4 ng for Pb. Raw U–Pb data were processed using the PBDAT program. Isochron regressions and weighted averages were calculated using the ISOPLOT program of Ludwig (1989, 1990). Calculating the isochron parameters, we took into account the errors reproducibility of 0.10, 0.15, and 0.20% for $^{206}Pb/^{204}Pb$, $^{207}Pb/^{204}Pb$, and $^{208}Pb/^{204}Pb$ ratios, respectively. These values are assessed by means of reiterated analyses of the BCR-1 standard. The Pb concentration in phases L-2 and L-3 of Sample 107/18 turned out to be extremely low, and Pb isotope ratios characterizing them are measured with greater uncertainty than in other cases. All uncertainty values are quoted in the text and Fig. 5 at the 2σ level.

RESULTS AND DISCUSSION

We studied the U–Pb systematics for eight "best" samples of the Malgina limestones, which were selected in accord with criteria described above, and also for samples 60/8 and 56/38, which show more noticeable signs of secondary alterations (see below). The analyzed sampling levels are indicated in the formation section (Fig. 2), and U–Pb data for studied carbonate phases are presented in the table. Samples collected at various levels of the section characterizing the eastern limb of the Gornostakhskii anticline (56/38, 56/39, 107/16, 107/17, 107/18, and 107/19) have higher U concentrations, greater $^{238}U/^{204}Pb$ ratios, and more radiogenic Pb isotope composition, than samples from

U–Pb data characterizing different carbonate phases of limestone samples from the Malgina Formation

Sample no.	Phase	Concentration, ppm		$\mu = {}^{238}U/{}^{204}Pb$	$^{206}Pb/^{204}Pb$	$^{207}Pb/^{204}Pb$	$^{208}Pb/^{204}Pb$
		Pb	U				
56/38	PCC-2	0.634	1.506	227	54.123	18.185	37.892
	L1	0.171			19.967	15.840	38.401
	L2	0.457			43.497	17.394	38.008
	L3	0.402			58.349	18.498	38.099
56/39	PCC-2	0.768	1.412	140.6	33.033	16.709	37.789
	L3	0.605			34.376	16.819	37.968
60/3	PCC-2	0.520	0.0613	7.64	19.271	15.658	39.059
	L2	0.346			19.100	15.683	38.938
	L3	0.634			19.255	15.657	39.012
	ISR	3.34			19.002	15.664	37.834
60/5	PCC-2	0.772	0.0916	7.72	19.549	15.686	39.095
60/8	PCC-2	1.661	0.1072	4.22	20.157	15.745	38.740
	L1	0.450	0.0484	6.70	18.525	15.339	37.214
	L2	0.780			20.452	15.742	39.316
	L3	0.833	0.0695	5.49	20.377	15.741	39.133
60/10	PCC-2	0.601	1.146	174.9	48.694	17.814	38.820
	L3	0.632			50.030	17.991	39.128
107/16	PCC-2	0.702	2.34	391	76.347	19.951	38.535
	L1	0.145			22.802	16.030	38.294
	L2	0.591			59.666	18.631	38.116
	L3	0.772			74.663	19.816	38.363
107/17	PCC-2	0.530			79.981	20.172	38.215
	L1	0.275	1.312	311	20.628	15.771	38.168
	L2	0.159	0.849	627	76.619	19.982	38.492
	L3	0.243	1.214	672	95.532	21.354	38.468
	ISR	3.38	1.454	42.1	55.682	19.168	37.548
107/18	PCC-2	0.991	4.17	743	140.98	24.633	38.379
	L1	0.059	3.38	450	34.835	16.728	38.126
	L2	0.496	3.35	1210	144.81 (3%)	24.790	35.058 (2%)
	L3	0.420	2.24	985	149.90 (1%)	25.298	38.430 (0.13%)
	ISR	37.9	28.6	77.8	61.677	18.914	37.842
107/19	PCC-2	0.906	2.42	237	46.263	17.687	38.011
	L3	0.877			48.745	17.900	38.174

the upper member of the section exposed at the western limb (60/3, 60/5, 60/8, and 60/10).

The established variations of Pb isotope ratios in different carbonate phases, which were obtained by the step leaching of "best" samples and those that experienced secondary alterations (60/8 and 56/38), are illustrated in Figs. 3 and 4. The data point that characterizes average isotopic parameters of Pb incoming from external contaminating sources (water, air, aerosol, and dust) during the sample treatment (Hirao and Patterson, 1974) is shown in these figures as well. The Pb isotope composition of blank runs in our laboratory is within the same uncertainty limits: $^{206}Pb/^{204}Pb = 17.945$, $^{207}Pb/^{204}Pb = 15.324$, $^{208}Pb/^{204}Pb = 37.159$.

As one can see from Figs. 3 and 4, Pb that enters the first acid leachate (phase L-1) corresponds in isotopic parameters to the mixture of leads from external contaminating sources and from secondary carbonate phase dissolved at this treatment stage. Consequently, we should ignore all L-1 phases of limestones by the Pb–Pb age calculation. Babinski *et al.* (1995, 1999)

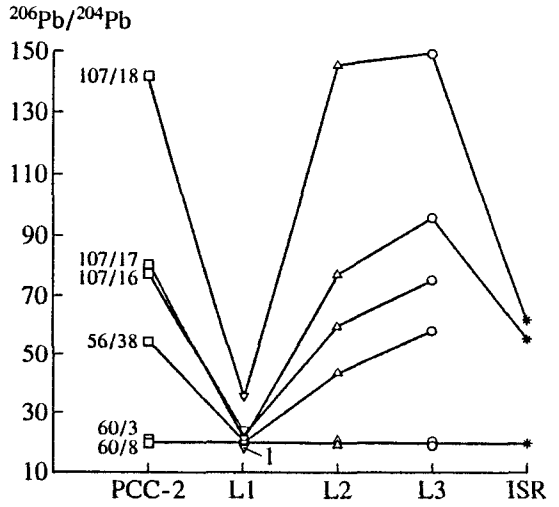

Fig. 3. Variation of $^{206}Pb/^{204}Pb$ ratios in carbonate and ISR phases of studied limestones. Data point 1 denotes the average $^{206}Pb/^{204}Pb$ ratio for external contaminating substances. Broken lines connect data points characterizing different phases of rock samples indicated by numbers at the left. Abbreviations indicating phases are explained in the text.

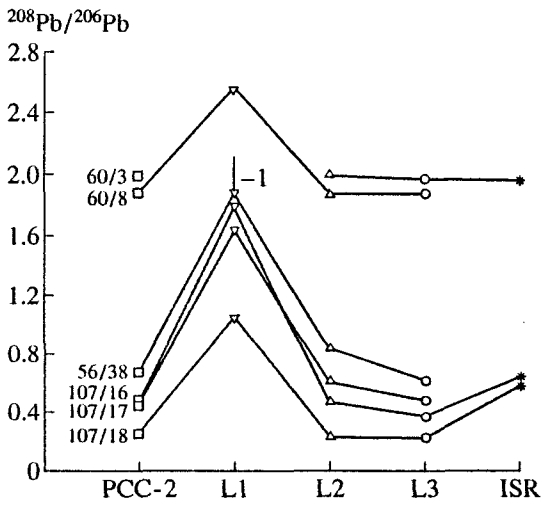

Fig. 4. Variation of $^{208}Pb/^{206}Pb$ ratios in carbonate and ISR phases of studied limestones. Data point 1 denotes the average $^{208}Pb/^{206}Pb$ ratio for external contaminating substances. Broken lines connect data points characterizing different phases of rock samples indicated by numbers at the left. Abbreviations indicating phases are explained in the text.

came to the same conclusion, when they studied Mesoproterozoic carbonate rocks in Brazil.

In samples from the eastern limb of the Gornostakhskii anticline, Pb in phases L-2 and L-3 is progressively more radiogenic than in corresponding weighings untreated in HBr. Apparently, the former are enriched in Pb of the early diagenetic carbonate and have a lower content of secondary carbonate material. As for Pb of silicate fractions (ISR phases), it is less radiogenic (beyond the measurement uncertainty) than in corresponding phases L-3. Accordingly, the carbonate phases successively leached from samples are either uncontaminated by Pb from associated siliciclastic material, or such a contamination is insignificant.

Samples 60/3 and 60/8 from the western anticline limb showed the comparable Pb isotope compositions almost in all their phases: in phase L-2 leached at the second stage, in phase L-3 enriched in primary carbonate, in phase PCC-2 leached by HCl from the whole rock samples, and even in insoluble residue (ISR phase). As compared to all other studied samples, limestones from this locality contain the least radiogenic Pb and show the lowest $^{238}U/^{204}Pb$ ratios, and we assume that the Pb isotope compositions in their carbonate and silicate fractions were equilibrated at the early diagenetic stage almost without the U gain. At the same time, the Pb concentration in Sample 60/8 that experienced considerable secondary alterations in terms of Rb–Sr systematics is noticeably greater than in other samples. It is likely therefore that post-diagenetic alterations were responsible for simultaneous Pb and Sr gain in this carbonate rock, the more so that the rock was sampled within a zone of irregular late dolomitization of the Malgina limestones along their contact with the Tsipanda Formation. Chaotic and irregular in shape areas of secondary dolomitization (Semikhatov and Serebryakov, 1983, Fig. 29) enable a suggestion that the less intense alterations interrelated with this process were also irregular in space and influenced Sample 60/8, but left intact others collected in the western limb of the Gornostakhskii anticline. Here, we should emphasize once again that data of cathodoluminescent analysis show that limestone samples from the site under consideration are recrystallized slightly stronger than in the eastern anticline limb, and that the recrystallization is of a distinct patchy character.

Sample 56/38 from the eastern anticline limb does not differ from other samples of this site in the trends of Pb isotope variations in various carbonate phases obtained by step leaching (Figs. 3 and 4). This sample is, however, comparatively depleted in Sr and shows the $^{87}Sr/^{86}Sr$ ratio that is higher than in neighboring samples collected 10 m above and 20 m below in the section. The relatively high degree of secondary alterations in this sample is also evident from distribution of data points characterizing its different phases, which significantly deviate from the strait line in Fig. 6. Taking into account all characteristics considered above, we excluded the results obtained for samples 60/8 and 56/38 from the data set used for the Pb–Pb age calculation.

In the $^{207}Pb/^{204}Pb$–$^{206}Pb/^{204}Pb$ diagram (Fig. 5), data points of L-2 and L-3 phases plot along a strait line within the sufficiently wide diapason of variables along

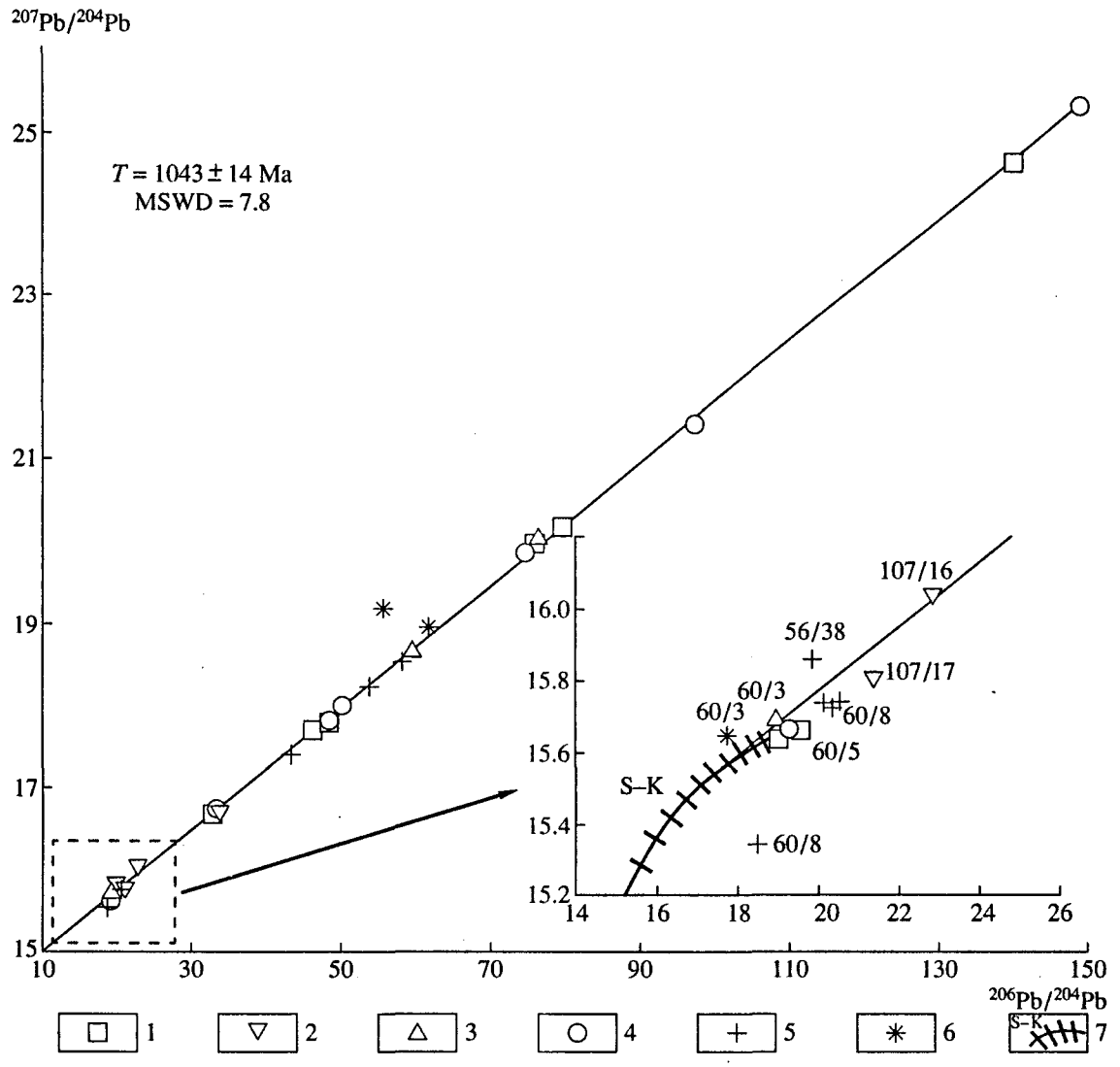

Fig. 5. $^{207}Pb/^{204}Pb$–$^{206}Pb/^{204}Pb$ diagram for limestones of the Malgina Formation: (1) PCC-2 phases; (2) L-1 phases; (3) L-2 phases; (4) L-3 phases; (5) all phases of samples 60/8 and 56/38; (6) ISR phases; (7) Pb accumulation curve, according to Stacey and Kramers (abbreviations are explained in the text).

both coordinate axes. The absence of correlation between Pb concentrations and $^{206}Pb/^{204}Pb$ ratios (see the table), and also between $^{208}Pb/^{204}Pb$ and $^{206}Pb/^{204}Pb$ ratios (Fig. 6), indicates that the regression in Fig. 5 is not the mixing line and has a geochronological meaning.

The Pb–Pb age calculated for seven data points characterizing L-3 phases, which are most enriched in primary (early diagenetic) carbonate material, is 1043 ± 38 Ma, MSWD = 13.5. For 13 data points of L-2 and L-3 phases, the calculated age equals 1048 ± 25 Ma, MSWD = 13. The regression line under consideration also approximates data points of bulk carbonate phases PCC-2, which were leached in HCl without treatment of samples in HBr. Consequently, despite possible effects of secondary alterations and laboratory contamination, these data points do not deviate from the errorchron to such an extent that would be greater than the summary experimental and geochemical uncertainty characterizing the regression line of primary carbonate phases. In this case, we can use PCC-2 phases for the Pb–Pb age calculation, thus having 18 data points defining the errorchron. The corresponding age value of 1043 ± 14 Ma (MSWD = 7.8) coincides, within the uncertainty limits, with the value calculated for seven carbonate phases of the Malgina limestones, which are enriched in primary carbonate material. The high MSWD value presumably is a consequence of the irregular, early diagenetic recrystallization of carbonate sediments.

Data considered above suggest an important conclusion. If the "best" samples are selected on the basis of

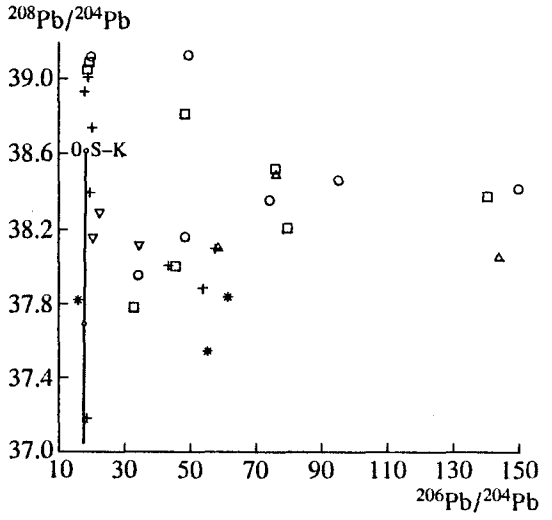

Fig. 6. $^{208}Pb/^{204}Pb$–$^{206}Pb/^{204}Pb$ diagram for limestones of the Malgina Formation (symbols as in Fig. 5).

strict geochemical criteria, the analysis of Rb–Sr systematic included, and if the share of non-cogenetic carbonate phases is small and insignificantly affecting the U–Pb characteristics of bulk carbonate material, then we can use PCC-2 phases, in addition to L-2 and L-3 phases, for the determination of Pb–Pb ages of carbonate rocks. In some cases, this offers a possibility to extend the variation diapason of measured Pb isotope ratios and to decrease the uncertainty of isotopic dating. This does not mean, however, that all whole rock samples of carbonates are suitable *a priori* for the direct Pb–Pb dating. First, we must test their appropriateness using the procedure of step leaching that allows us to separate primary and secondary carbonate phases, and to determine the degree of U–Pb system disturbance in carbonate rocks.

CONCLUSION

The Pb–Pb age value of 1043 ± 14 Ma calculated for the Malgina Formation is consistent with its stratigraphic position in the terminal Middle Riphean horizons and with isotopic dates, which are known for underlying and overlying Riphean subdivisions of the Uchur–Maya region and have been obtained using the U–Pb dating of zircon and baddeleyite (Rainbird *et al.*, 1998; Khudoley *et al.*, 1999, 2001). Among these dates, there is as well the Pb–Pb age of 1025 ± 40 Ma obtained for limestones of the lower Lakhanda Group (Neryuen Formation), which are located stratigraphically higher than the Malgina Formation.

Distribution of available isotopic dates in the section shows that thick carbonate successions representing an upper part of the Kerpyl Group and the whole Lakhanda Group accumulated during the comparatively short geological period of about 50–60 m.y. long. Together with the Middle Riphean Yusmastakh formation of the Anabar massif (Gorokhov *et al.*, 2001), these successions exemplify the quick accumulation of thick deposits on the Riphean carbonate platforms of Siberia.

In the context of this study, it is interesting to compare the aforementioned Pb–Pb ages of two carbonate formations of the Uchur–Maya region with the date of 1035 ± 60 Ma that was obtained earlier for dolomites and limestones of the Sukhaya Tunguska Formation exposed in the Turukhansk region of central Siberia (Ovchinnikova *et al.*, 1995). Paleontological and C-isotope chemostratigraphic data (Semikhatov and Serebryakov, 1983; Semikhatov, 1995; Knoll *et al.*, 1995; Podkovyrov and Vinogradov, 1996; Vinogradov *et al.*, 1998; Sergeev, 1999; Bartley *et al.*, 2001) show that the Sukhaya Tunguska Formation is terminal one in the Middle Riphean succession of the last region and occurs between stratigraphic analogues of the Malgina Formation and lower part of the Lakhanda Group of the Uchur–Maya region (Semikhatov *et al.*, 2000; Bartley *et al.*, 2001).

Accordingly, we have the following successive values of Pb–Pb ages characterizing stratigraphic succession of three Riphean formations (from the base upward): 1043 ± 14 Ma (Malgina Formation), 1035 ± 60 Ma (Sukhaya Tunguska Formation), and 1025 ± 40 Ma (Neryuen Formation of the Lakhanda Group). In terms of formal statistical criteria, difference between these dates is insignificant. At the same time, it is obvious that we have a series of values (probabilistic averages) diminishing in stratigraphic succession. Moreover, this series as a whole and each particular value are concordant with isotopic dates obtained by other methods.

This is a first known series of stratigraphically successive Pb–Pb dates obtained for carbonate rocks and characterizing the accumulation (early diagenesis) time of successive Upper Precambrian formations. Outside Siberia, this series can be continued by dates known in the southern Urals, namely by the isochron Pb–Pb age of 836 ± 25 Ma that is obtained for limestones of the Inzer Formation distinguished in the lower part of the Upper Riphean stratotype (Ovchinnikova *et al.*, 1998), and by the weighted average value of 780 ± 85 Ma that characterizes Pb–Pb ages of the Min'yar dolomites occurring in the upper part of the stratotype (Ovchinnikova *et al.*, 2000). Like in Siberia, both Pb–Pb ages of Riphean carbonate deposits in the Urals are consistent with dating results obtained for corresponding formations by other methods. Thus, despite a considerable analytical uncertainty of the method, the Pb–Pb dating of carbonate rocks is of reasonable resolution ability and can be informative with respect to the accumulation history of Riphean formations.

In order to obtain the isochron Pb–Pb ages of stratigraphic significance, it is necessary however to use the outlined strict procedure of selecting carbonate rock samples potentially appropriate for dating and to apply the step leaching to selected samples that removes sec-

ondary carbonate phases (and sulfide admixture, when needed). Using the leaching method, we avoid the systematic inaccuracy of age determinations that is related to involvement of age-variable carbonate phases having different U–Pb parameters in the isotopic analysis.

ACKNOWLEDGMENTS

We are grateful to A.G. Rublev and Yu.D. Pushkarev whose comments were used to improve the manuscript, and to A.B. Kuznetsov for the constructive discussion of the obtained results and for his assistance in preparation of illustrative materials. We also thank I.V. Kislova who analyzed the Fe and Mn distribution in limestone samples from the Malgina Formation. The work was supported by the Russian Foundation for Basic Research, project nos. 99-05-65181, 99-05-64054, and 00-05-72011.

Reviewers Yu.D. Pushkarev and A.G. Rublev

REFERENCES

Asmerom, I. and Jacobsen, S.B., The Pb Isotopic Evolution of the Earth: Inferences From River Water Suspended Loads, *Earth Planet. Sci. Lett.*, 1993, vol. 115, no. 1/4, pp. 245–256.

Babinski, M., Chemale, F., Jr., and Van Schmus, W.R., The Pb–Pb Age of the Minas Supergroup Carbonate Rocks, Quadrilatero Ferrifero, Brazil, *Precambrian Res.*, 1995, vol. 72, no. 3/4, pp. 235–245.

Babinski, M., Van Schmus, W.R., and Chemale, F., Jr., Pb–Pb Dating and Pb Isotope Geochemistry of Neoproterozoic Carbonate Rocks From the Sao Francisco Basin, Brazil: Implications for the Mobility of Pb Isotopes during Tectonism and Metamorphism, *Chem. Geol.*, 1999, vol. 160, no. 2, pp. 175–199.

Banner, J.K. and Hanson, G.N., Calculation of Simultaneous Isotopic and Trace Element Variations during Water-Rock Interaction with Applications to Carbonate Diagenesis, *Geochim. Cosmochim. Acta*, 1990, vol. 54, no. 11, pp. 3123–3137.

Bartley, J.K., Semikhatov, M.A., Kaufman, A.J., *et al.*, Global events across the Mesoproterozoic–Neoproterozoic boundary: C and Sr Isotopic Evidence from Siberia, *Precambrian Res.*, 2001, vol. 111, pp. 165–202.

Brand, U. and Veizer, J., Chemical Diagenesis of a Multicomponent Carbonate System. 2. Stable Isotopes, *J. Sediment. Petrol.*, 1981, vol. 51, no. 3, pp. 987–997.

Brasier, M.D. and Lindsay, J.F., A Billion Years of Environmental Stability and the Emergence of Eukaryotes: New Data From Northern Australia, *Geology*, 1998, vol. 26, no. 5, pp. 555–558.

Derry, L.A., Kaufman, A.J., and Jacobsen, S.B., Sedimentary Cycling and Environmental Change in the Late Proterozoic: Evidence From Stable and Radiogenic Isotopes, *Geochim. Cosmochim. Acta*, 1992, vol. 56, no. 3, pp. 1317–1329.

Geokhronologiya dokembriya Sibirskoi platformy i ee skladchatogo obramleniya (Geochronology of the Precambrian in the Siberian Platform and Surrounding Folded Structures), Manuilova, M.M., Ed., Leningrad: Nauka, 1968.

Gerling, E.K. and Iskanderova, A.D., Pb–Pb Isochron Dating of Carbonate Rocks as Applied to Recognition of Early Metamorphic Stages, in *Aktual'nye voprosy sovremennoi geokhronologii* (Urgent Problems of Modern Geochronology), Moscow: Nauka, 1976, pp. 224–231.

German, T.N., *Organicheskii mir milliard let nazad* (Organic World a Billion Years Ago), Leningrad: Nauka, 1990.

Gobeil, C. and Silverberg, N., Diagenesis of Lead in Laurentian Trough Sediments, *Geochim. Cosmochim. Acta*, 1989, vol. 53, no. 8, pp. 1889–1895.

Gorokhov, I.M., Diagenesis of Carbonate Sediments: Behavior of Trace Elements and Strontium Isotopes, in *Litologiya i paleogeografiya. Vyp. 4* (Lithology and Paleogeography, Issue 4), Verba, Yu.L., Ed., St. Petersburg: St. Petersburg Gos. Univ., 1996, pp. 141–164.

Gorokhov, I.M., Mel'nikov, N.N., Turchenko, T.L., and Kutyavin, E.P., Rb–Sr Systematics of Pelitic Fractions of the Lower Riphean Shales, The Ust' Il'ya Formation of the Anabar Massif, Northern Siberia, *Litol. Polezn. Iskop.*, 1997, no. 5, pp. 530–539.

Gorokhov, I.M., Semikhatov, M.A., Baskakov, A.V., *et al.*, Sr Isotopic Composition in Riphean, Vendian, and Lower Cambrian Carbonates from Siberia, *Stratigr. Geol. Korrelyatsiya*, 1995, vol. 3, no. 1, pp. 3–33.

Gorokhov, I.M., Semikhatov, M.A., Mel'nikov, N.N., *et al.*, Rb–Sr Geochronology of Middle Riphean Shales, the Yusmastakh Formation of the Anabar Massif, Northern Siberia, *Stratigr. Geol. Korrelyatsiya*, vol. 9, no. 3, pp. 3–28.

Gorokhov, I.M., Semikhatov, M.A., Trubetskoi, E.R., *et al.*, Rb–Sr and K–Ar Ages of the Lower Riphean Sedimentary Geochronometers from the Anabar Massif, *Izv. Akad. Nauk SSSR, Ser. Geol.*, 1991, no. 7, pp. 17–32.

Hirao, Y. and Patterson, C.C., Lead Aerosol Pollution in the Sierra Overrides. Natural Mechanism Which Exclude Lead From Food Chain, *Science*, 1974, vol. 184, no. 4140, pp. 989–1002.

Hoff, J.A., Jemerson, J., and Hanson, J.N., Application of Pb Isotopes to the Absolute Timing of Reginald Exposure Events in Carbonate Rocks: An Example From U-Rich Dolostones From the Wahoo Formation (Pennsylvanian), Prude Bay, Alaska, *J. Sediment. Res.*, 1995, vol. 65, no. 1, pp. 225–233.

Jahn, B.-M. and Cuvellier, H., Pb–Pb and U–Pb Geochronology of Carbonate Rocks: An Assessment, *Chem. Geol. (Isot. Geosci. Sect.)*, 1994, vol. 115, no. 1/2, pp. 125–151.

Jahn, B.-M. and Simonson, B.M., Carbonate Pb–Pb Ages of the Wittenoom Formation and Carawine Dolomite, Hamersley Basin, Western Australia (with Implications for Their Correlation with the Transvaal Dolomite of South Africa), *Precambrian Res.*, 1995, vol. 72, no. 3/4, pp. 247–261.

Jahn, B.-M., Bertrand-Sarfati, J., Morin, N., and Mace, J., Direct Dating of Stromatolitic Carbonates From the Schmidtsdrif (Transvaal Dolomite), South Africa, with Implication on the Age of the Ventersdorp Supergroup, *Geology*, 1990, vol. 18, no. 12, pp. 1211–1214.

Jones, C.E., Halliday, A.N., and Lohmann, K.C., The Roles of Primary Mineralogy and Diagenetic Alteration in the Application of U–Pb Dating to Limestones, *Am. Geophys. Union. Fall Meeting*, October 27, 1992, *Supplement to EOS*, 1992, pp. 32–47.

Kah, L.C., Sherman, A.G., Narbonne, G.M., *et al.*, ^{13}C Stratigraphy of the Proterozoic Bylot Supergroup, Baffin Island, Canada: Implications for Regional Lithostratigraphic Correlation, *Canad. J. Earth Sci.*, 1999, vol. 36, no. 3, pp. 313–332.

Khudolei, A.K., Reinbird, R., Stern, R., *et al.*, New Data on Riphean Tectogenesis in Northeastern Russia, in *Tektonika, geodinamika i protsessy magmatizma i metamorfizma. Materialy soveshchaniya. T. II* (Proc. of Conference: Tectonics, Geodynamics, and Processes of Magmatism and Metamorphism), 1999, pp. 261–264.

Khudoley, A.K., Rainbird, R.M., Stern, R.A., *et al.*, Sedimentary Evolution of the Riphean–Vendian Basin of Southeastern Siberia, *Precambrian Res.*, 2001, vol. 111, nos. 1–4, pp. 235–256.

Knoll, A.H. and Semikhatov, M.A., The Genesis and Time-Distribution of Two Distinctive Proterozoic Stromatolite Microstructures, *Palaios*, 1998, vol. 13, no. 4, pp. 408–422.

Knoll, A.H., Kaufman, A.J., and Semikhatov, M.A., The Carbon-Isotopic Composition of Proterozoic Carbonates: Riphean Succession From Northwestern Siberia (Anabar Massif, Turukhansk Uplift), *Am. J. Sci.*, 1995, vol. 295, pp. 823–850.

Komar, V.A., *Stromatolity verkhnedokembriiskikh otlozhenii severa Sibirskoi platformy i ikh stratigraficheskoe znachenie* (Stromatolites from Upper Precambrian Deposits of the North Siberian Platform and Their Stratigraphic Significance), Moscow: Nauka, 1966.

Krylov, I.N., *Stromatolity rifeya i fanerozoya SSSR* (Riphean and Phanerozoic Stromatolites of the USSR), Moscow: Nauka, 1975.

Kuznetsov, A.B., Gorokhov, I.M., Semikhatov, M.A., *et al.*, Sr Isotope Composition in Limestones of the Inzer Formation, the Upper Riphean Stratotype of Southern Urals, *Dokl. Ross. Akad. Nauk*, 1997, vol. 353, no. 2, pp. 249–254.

Litologiya i neftegazonosnost' yugo-vostoka Sibirskoi platformy (verkhnii dokembrii) (Lithology and Petroliferous Potential of the Southeastern Siberian Platform), Moscow: Nauka, 1980.

Ludwig, K.R., Isoplot for MS-DOS. A Plotting and Regression Program for Radiogenic Isotope Data for IBM-PC Compatible Program Computers. Version 2.00, *US Geol. Surv. Open File Rep. 88-557*, 1990.

Ludwig, K.R., PBDAT for MS-DOS. A Computer Program for IBM-PC Compatibles for Processing Row Pb–U–Th Isotope Data. Version 1.06. *US Geol. Surv. Open File Rep. 88-542*, 1989.

Maliva, R.G., Knoll, A.H., and Seiver, R., Secular Change in Chert Distribution: a Reflection of Evolving Biological Participation in the Silica Cycle, *Palaios*, 1989, vol. 4, no. 5, pp. 519–532.

Manhes, G., Minster, J.E., and Allegre, C.J., Comparative Uranium–Thorium–Lead and Rubidium–Strontium Study of the Severin Amphoterite: Consequences for Early Solar System Chronology, *Earth Planet. Sci. Lett.*, 1978, vol. 39, no. 1, pp. 14–24.

Moorbath, S., Taylor, P.N., Orpen, J.L., *et al.*, First Direct Radiometric Dating of Archaean Stromatolite Limestone, *Nature*, 1987, vol. 326, no. 6116, pp. 865–867.

Nuzhnov, S.V., *Rifeiskie otlozheniya yugo-vostoka Sibirskoi platformy* (Riphean Deposits in the Southeastern Siberian Platform), Moscow: Nauka, 1967.

Ovchinnikova, G.V., Semikhatov, M.A., Gorokhov, I.M., *et al.*, U–Pb Systematics of Precambrian Carbonates, the Riphean Sukhaya Tunguska Formation of the Turukhansk Uplift in Siberia, *Litol. Polezn. Iskop.*, 1995, no. 5, pp. 525–536.

Ovchinnikova, G.V., Vasil'eva, I.M., Semikhatov, M.A., *et al.*, U–Pb Systematics on Proterozoic Carbonate Rocks: The Inzer Formation of the Upper Riphean Stratotype (Southern Urals), *Stratigr. Geol. Korrelyatsiya*, 1998, vol. 6, no. 4, pp. 20–31.

Ovchinnikova, G.V., Vasil'eva, I.M., Semikhatov, M.A., *et al.*, The Pb–Pb Trail Dating of Carbonates with Open U–Pb Systems: The Min'yar Formation of the Upper Riphean Stratotype, Southern Urals, *Stratigr. Geol. Korrelyatsiya*, 2000, vol. 8, no. 6, pp. 3–19.

Petrov, P.Yu., Clay–Carbonate Sedimentation Cycle and Development of Carbonate Platform: The Linok Formation of the Middle Riphean, Turukhansk Uplift of Siberia, *Litol. Polezn. Iskop.*, no. 3, pp. 268–289.

Podkovyrov, V.N. and Vinogradov, D.P., Epigenesis and Safety of C and O isotopic Systems in Carbonates of the Lakhanda and Yudoma Groups, the Upper Riphean–Vendian Sections at the Belaya River (SE Yakutia), *Litol. Polezn. Iskop.*, 1996, no. 5, pp. 541–551.

Rainbird, R.H., Stern, R.A., Khudoley, A.K., *et al.*, U–Pb Geochronology of Riphean Supracrustal Rocks From Southeastern Siberia and Its Bearing on the Laurentia–Siberia Connection, *Earth Planet. Sci. Lett.*, 1998, vol. 164, pp. 409–420.

Russell, J., Chadwick, B., Krishna Rao, B., and Vasudiv, V.N., Whole-Rock Pb–Pb Isotopic Ages of Late Archean Limestones, Karnataka, India, *Precambrian Res.*, 1996, vol. 78, no. 4, pp. 261–272.

Semikhatov, M.A., Methodic Principles of the Riphean Stratigraphy, *Stratigr. Geol. Korrelyatsiya*, 1995, vol. 3, no. 6, pp. 33–50.

Semikhatov, M.A. and Serebryakov, S.N., *Sibirskii gipostratotip rifeya* (Siberian Hypostratotype of the Riphean), Moscow: Nauka, 1983.

Semikhatov, M.A., Gorokhov, I.M., Kutyavin, E.P., *et al.*, Potentialities of Sedimentary Geochronometers: the Riphean Totta Formation of East Siberia as an Example, *Litol. Polezn. Iskop.*, 1989, no. 6, pp. 3–18.

Semikhatov, M.A., Ovchinnikova, G.V., Gorokhov, I.M., *et al.*, Isotopic Age of the Middle–Upper Riphean Boundary: the Pb–Pb geochronology of Carbonate Rocks of the Lakhanda Group, the Eastern Siberia, *Dokl. Ross. Akad. Nauk*, 2000, vol. 372, no. 2, pp. 216–221.

Sergeev, V.N., Silicified Microfossils From Transitional Meso-Neoproterozoic Deposits of the Turukhamsk Uplift, Siberia, *Bull. Soc. Paleontol. It.*, 1999, vol. 38, nos. 2–3, pp. 287–295.

Shenfil', V.Yu., *Pozdnii dokembrii Sibirskoi platformy* (Late Precambrian in the Siberian Platform), Novosibirsk: Nauka, 1991.

Stratigraficheskaya skhema rifeiskikh i vendskikh otlozhenii Volgo-Ural'skoi oblasti. Ob"yasnitel'naya zapiska (Stratigraphic Scheme of Riphean and Vendian Deposits in the Volga–Ural Region, Explanatory Notes), Ufa: IG UNTs, Ross. Akad. Nauk, 2000.

Timofeev, B.V., German, T.N., and Mikhailova, N.S., *Mikrofitofossilii dokembriya, kembriya i ordovika* (Microfossils of the Precambrian, Cambrian, and Ordovician), Leningrad: Nauka, 1976.

Toulkeridis, T., Goldstein, S.L., Clauer, N., *et al.*, Sm–Nd, Rb–Sr and Pb–Pb Dating of Silicic Carbonates From the Early Archaean Barberton Greenstone Belt, South Africa. Evidence for Post-Depositional Isotopic Resetting at Low Temperature, *Precambrian Res.*, 1998, vol. 92, pp. 129–144.

Vasil'eva, I.M., Ovchinnikova, G.V., Gorokhov, I.M., *et al.*, Method of Separation (Concentration) of Primary and Sec-

ondary Carbonates in the Pb–Pb Geochronology, Abstracts of Papers, *Soveshchanie: Osadochnye formatsii dokembriya i ikh rudonosnost'* (Conf. on Precambrian Sedimentary Formations and Their Mineral Resources), St. Petersburg, 1998, pp. 8–9.

Vasil'eva, I.M., Ovchinnikova, G.V., Semikhatov, M.A., *et al.*, Pb–Pb Age of Limestones from the Malgina Formation, the Kerpyl' Group of the Middle Riphean, East Siberia, Abstracts of Papers, *1-aya Rossiiskaya konferentsiya po izotopnoi geokhronologii* (1st Russian Conf. on Isotopic Geochronology), Moscow, 2000, pp. 82–84.

Veis, A.F. and Vorob'eva, N.G., Riphean and Vendian Microfossils of the Anabar Massif, *Izv. Akad. Nauk SSSR, Ser. Geol.*, 1992, no. 1, pp. 114–130.

Veis, A.F. and Vorob'eva, N.G., Microbiotas of the Kerpyl' Group in the Riphean Hypostratotype of Siberia, *Stratigr. Geol. Korrelyatsiya*, 1993, vol. 1, no. 1, pp. 41–58.

Veis, A.F., Larionov, N.N., Vorob'eva, N.G., and Lee Seong-Joo, Significance of Microfossils for Riphean Stratigraphy of the Southern Urals (Bashkirian Meganticlinorium) and Adjacent Region (Kama-Belaya Aulacogen), *Stratigr. Geol. Korrelyatsiya*, vol. 8, no. 5, pp. 3–28.

Veis, A.F., Petrov, P.Yu., and Vorob'eva, N.G., Transformations in Facies-Ecological Structure of Precambrian Biotas and Riphean Stratigraphy, *Geol. Geofiz.*, 1998, vol. 39, no. 1, pp. 85–96.

Vinogradov, V.I., Pokrovskii, B.G., Golovin, D.I., *et al.*, Isotopic Evidence of Epigenetic Alterations and Age Problem Concerning Riphean Deposits in the Uchur–Maya Region of East Siberia, *Litol. Polezn. Iskop.*, 1998, no. 6, pp. 629–646.

Whiterhouse, M.J. and Russell, J., Isotopic Systematics of Precambrian Marbles From the Lewisian Complex of Northwest Scotland: Implications for Pb–Pb Dating of Metamorphosed Carbonates, *Chem. Geol. (Isotop. Geosci. Sect.)*, 1997, vol. 136, no. 3/4, pp. 295–307.

Winter, B.L. and Johnson, C.M., U–Pb Dating of a Carbonate Subaerial Exposure Event, *Earth Planet. Sci. Lett.*, 1995, vol. 131, no. 1/2, pp. 177–187.

Yankauskas, T.V., Mikhailova, N.S., German, T.N., *et al.*, *Mikrofossilii dokembriya SSSR* (Precambrian Microfossils of the USSR), Moscow: Nedra, 1989.

Zachariah, J.K., Bhaskar Rao, Y.J., Srinivasan, R., and Gopalan, K., Pb, Sr and Nd Isotope Systematics of Uranium Mineralized Stromatolitic Dolomites From the Proterozoic Cuddapah Supergroup, South India: Constraints on Age and Provenance, *Chem. Geol.*, 1999, vol. 162, pp. 49–64.